



Adam Causse

Modeling and simulation of A320/A320neo ribs

Faculty of Engineering and Applied Sciences
Aerospace computational Engineering

MSc
Academic Year: 2025–2026

Supervisors: Dr Teschner T.
August 2025



Faculty of Engineering and Applied Sciences
Aerospace computational Engineering

MSc

Academic Year: 2025–2026

Adam Causse

Modeling and simulation of A320/A320neo ribs

Supervisors: Dr Teschner T.
August 2025

This thesis is submitted in partial fulfilment of the
requirements for the degree of MSc.

© Cranfield University 2025. All rights reserved. No part of
this publication may be reproduced without the written
permission of the copyright owner.

Academic Integrity Declaration

I declare that:

- the thesis submitted has been written by me alone.
- the thesis submitted has not been previously submitted to this university or any other.
- that all content, including primary and/or secondary data, is true to the best of my knowledge.
- that all quotations and references have been duly acknowledged according to the requirements of academic research.

I understand that knowingly submit work in violation of the above statement will be considered by examiners as academic misconduct.

Abstract

This study presents a simplified modeling of an A320neo using OpenVSP, enabling the determination of the rib profile supporting the engine. An FEA simulation is then performed to compare the structural behavior of a rib carrying a CFM-56 engine with that of a rib carrying a LEAP-1A. The results show that the rib designed for the LEAP-1A is approximately 25% heavier, highlighting the structural impact of integrating the newer, larger engine.

Keywords:

A320/A320Neo, Nervure, FEA simulation, CFM-56, Leap 1-A

Acknowledgements

I express my sincere gratitude to my professor for the knowledge, guidance, and support they have provided throughout this project and during our time in the program.

Dr. Tom-Robin Teschner

Contents

Academic Integrity Declaration	i
Abstract	ii
Acknowledgements	iii
Contents	iv
List of Figures	vi
List of Tables	vii
List of Abbreviations	viii
1 Introduction	1
2 Literature review	2
3 Methodology	3
3.1 3D modelisation of the aircraft	3
3.1.1 Use of the fuselage object	4
3.1.2 Use of the wing object	5
3.2 Ribs and spars modeling on CATIA	7
3.3 Rib design	8
4 FEA simulation and results	9
4.1 simulation setup	9
4.1.1 Material used	9
4.1.2 Loads calculation	10
4.1.3 Mesh size	10
4.2 Simulation and Optimization Results	11
4.2.1 Results and Optimization for the CFM-56 Engine	11
4.2.2 Results and Optimization for the LEAP-1A Engine	13
4.3 Dimension Standardization for Manufacturing	14
4.3.1 Rib Supporting the LEAP-1A Engine	14
4.3.2 Rib Supporting the CFM-56 Engine	16

5 Conclusion	17
5.1 Conclusion	17
References	18

List of Figures

3.1	A320 scheme	3
3.2	A320 Fuselage	4
3.3	A320 engine	4
3.4	A320 airfoils profiles	5
3.5	A320 wing model	5
3.6	Horizontal stabilizer of the A320	5
3.7	Front view of the A320	6
3.8	Left view of the A320	6
3.9	Wing shape on CATIA	7
3.10	Wing structure with supporting rib highlighted	7
3.11	rib with the starting parameters	8
4.1	Model prepared for the FEA	10
4.2	Von Mises criterion for CFM-56 engine rib	11
4.3	Rib design after opimization for the CFM-56	12
4.4	Von mises criterion for a Leap-1A engine rib	13
4.5	Rib design after opimization for the Leap-1A	14
4.6	Von mises criterion after standardization for Leap-1A engine rib	15
4.7	Rib design after standardization for the Leap-1A	15
4.8	Von mises criterion after standardization of the CFM-56 engine rib	16

List of Tables

3.1	Rib and stiffener parameters	8
4.1	Material properties of Aluminum 2024[1]	9
4.2	Rib characteristics used for optimization	11
4.3	Optimized rib characteristics for the CFM-56 engine	12
4.4	Initial rib characteristics for optimization of the LEAP-1A engine	13
4.5	Optimized rib characteristics for the LEAP-1A engine	13
4.6	Standardized rib dimensions for the LEAP-1A engine	14
4.7	Standardized rib dimensions for the CFM-56 engine	16

List of Abbreviations

MTOW	Maximum take-off weight
FEA	Finite Element Analysis

Chapter 1

Introduction

In September 2025, Airbus's A320 family remained the best-selling commercial aircraft range worldwide, with nearly 12,000 units delivered. As part of the continuous improvement of this highly successful product line, Airbus introduced the A320neo in 2016, featuring larger and more fuel-efficient engines. However, the increased mass and dimensions of these new powerplants require several structural adaptations, particularly in the wing–engine integration.

One of the components most directly affected by this change is the rib supporting the engine pylon. The transition from the CFM-56 to the LEAP-1A engine leads to higher loads and modified geometric constraints, prompting a redesign of the rib to ensure adequate structural strength and stiffness.

The aim of this study is to analyze the structural implications of this redesign. A simplified A320neo model is developed using OpenVSP to extract the geometry of the engine-supporting rib, followed by Finite Element Analysis (FEA) to compare the structural response of ribs designed for the CFM-56 and the LEAP-1A engines.

Chapter 2

Literature review

The A320neo wing employs a custom supercritical airfoil developed by Airbus engineers, which is not publicly available. However, several studies have proposed models to approximate it. Aldana and Riaz[2], for instance, use a modeling approach based on three supercritical airfoils to represent the A320 wing.

Magrini, Benini, Yao, Postma, and Sheaf[3] have conducted a comprehensive review of the challenges associated with adapting new ultra-high bypass ratio (UHBR) engines to existing aircraft platforms.

Chapter 3

Methodology

3.1 3D modelisation of the aircraft

To model the A320, we will use the scheme provided in the specifications[4]. We will then place them as background images using the background tool.

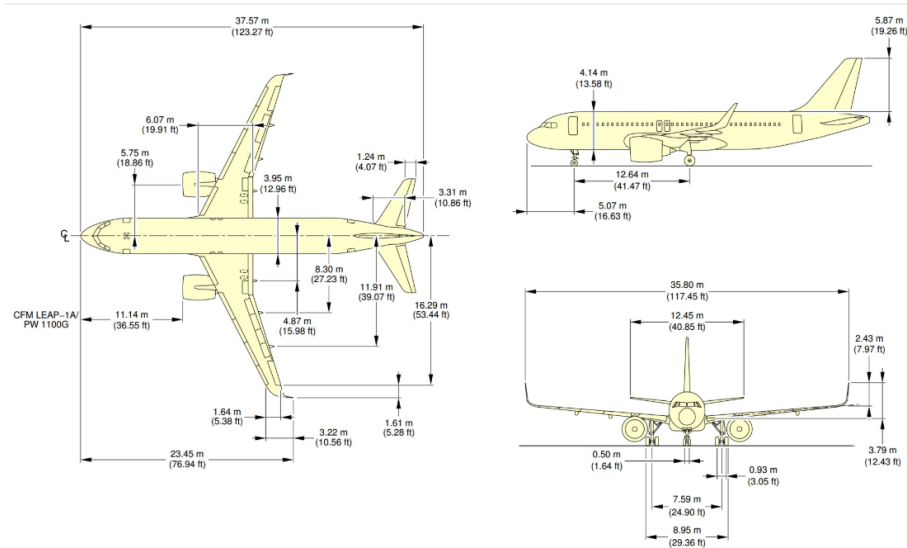


Figure 3.1: A320 scheme

3.1.1 Use of the fuselage object

The fuselage and engines are modeled using the fuselage object in OpenVSP. For the fuselage, six sections are defined to match the overall shape of the aircraft.

For the engines, a fuselage-type component is used in loop mode, creating a cylinder with internal and external sections. In this study, four internal sections and four external sections are defined to form the engine. Symmetry about the aircraft's longitudinal axis is then applied to generate the second engine.



Figure 3.2: A320 Fuselage

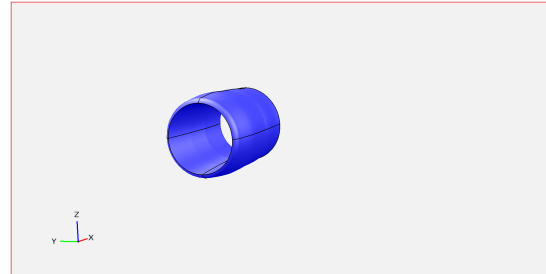


Figure 3.3: A320 engine

3.1.2 Use of the wing object

To model the wings and tail assembly of the aircraft, we use the wing object from Open Vsp. To define the wing profiles, we used the profiles proposed by Aldana and Riaz[2].

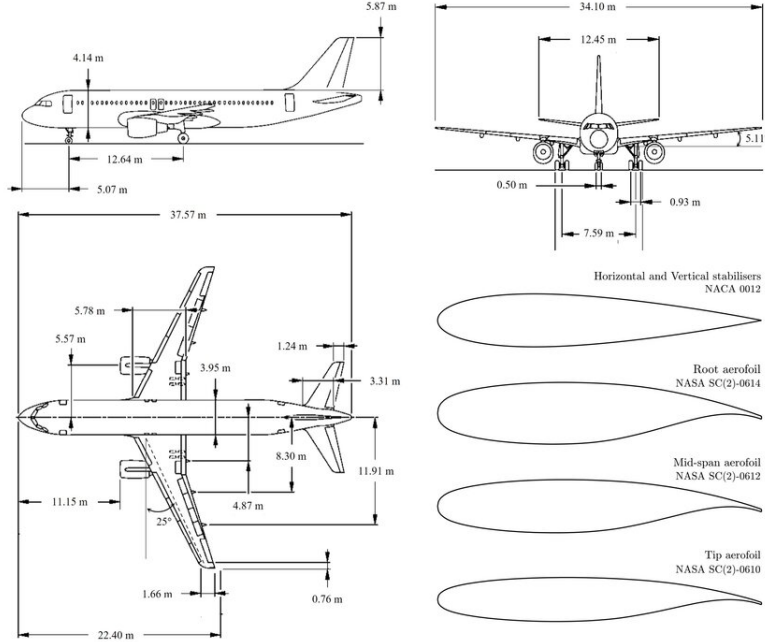


Figure 3.4: A320 airfoils profiles

For the main wing, the first airfoil profile is applied at the start of the first section, the second profile at the start of the second section, and the last profile at the start of the fourth section.

The sweep angle of 26° and the dihedral angle of 5° are derived from the modeling, using the scheme in Figure 3.1 as a reference in the background.

The modeling of the horizontal and vertical stabilizers is performed using the same method. Here, a single section is required with the NACA 0012 airfoil proposed by Aldana and Riaz[2].

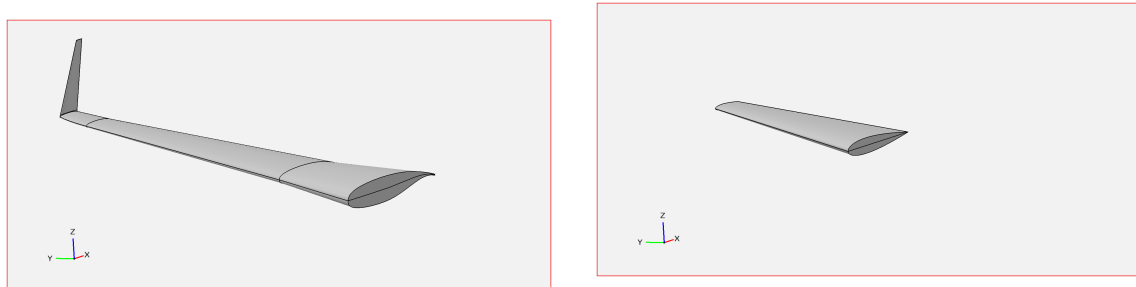


Figure 3.5: A320 wing model

Figure 3.6: Horizontal stabilizer of the A320

Once all these components are assembled, the complete A320 model is obtained.



Figure 3.7: Front view of the A320

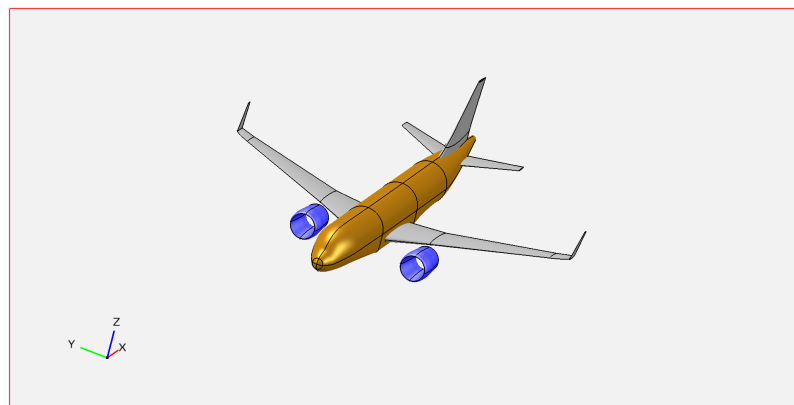


Figure 3.8: Left view of the A320

3.2 Ribs and spars modeling on CATIA

The right wing of the 3D model is exported to CATIA. The spars and ribs are created using the Generative Shape Design tool. The front spar is inclined at 26° following the wing sweep angle, while the rear spar, modeled as a single piece to simplify the wing design, has an inclination of 21° .

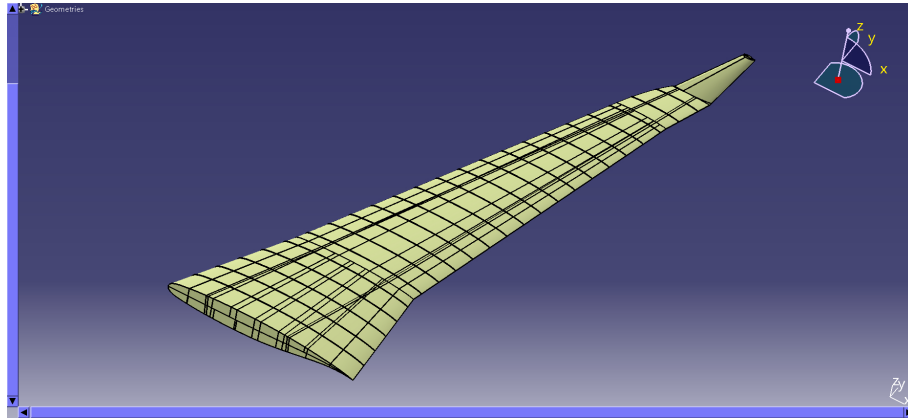


Figure 3.9: Wing shape on CATIA

Including the root rib and tip rib, there are 24 ribs per wing. They were left parallel to the fuselage as this has little impact on the rest of the study. The rib chosen for the remainder of the study is determined using the scheme in Figure 3.1. This is marked in red in the following figure.

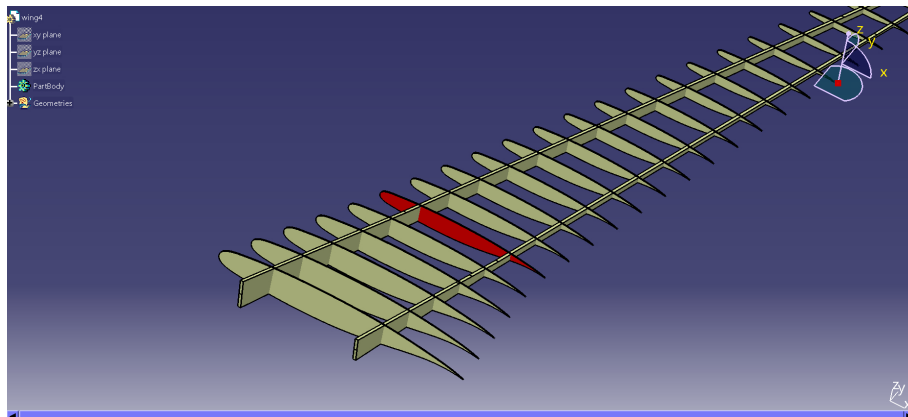


Figure 3.10: Wing structure with supporting rib highlighted

3.3 Rib design

The wing airfoil at the rib location is first extracted to enable a detailed structural study. The rib thickness and the space allocated for the spars are determined based on the methodology presented by Muhammad Amir Mirza Bin Mohd Zakuan, Abdul Aabid, and Sher Afghan Khan[5]. Accordingly, the rib thickness is set to 200mm, which serves as a parameter for subsequent optimization. The placement of stiffeners and holes is then defined following the schematic provided in the design specifications[4].

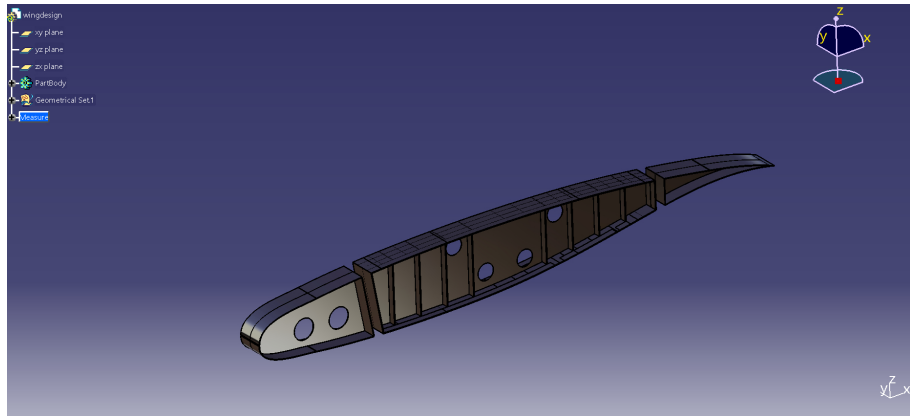


Figure 3.11: rib with the starting parameters

Rib thickness	200 mm
Top/bottom thickness	5 mm (*)
Stiffener thickness	5 mm (*)
Stiffener length	60 mm
Stiffener gap	200 mm
Central plate thickness	20 mm
Hole diameter	120 mm
Mass	90 kg

Table 3.1: Rib and stiffener parameters

The values marked with (*) in Table 3.1 are manually adjustable parameters. For this study, three rib configurations are evaluated: the first with these values set to 5mm, the second to 4mm, and the third to 3mm. These ribs serve as the baseline models for the subsequent analysis of both the CFM-56 and LEAP-1A engines.

Chapter 4

FEA simulation and results

4.1 simulation setup

For both simulations, the rib components are clamped on the faces in contact with the spars, while the central plate is subjected to distributed forces.

4.1.1 Material used

The material selected is Aluminum 2024, commonly used in aerospace applications due to its favorable balance between mass and strength. The properties used in this study are listed in Table 4.1.

Aluminum type	2024
Young's Modulus	73 GPa
Poisson's ratio	0.33
Density	2780 kg/m ³
Yield Strength	330 MPa

Table 4.1: Material properties of Aluminum 2024[1]

4.1.2 Loads calculation

According to Airbus[6], the maximum take-off weight (MTOW) of the A320neo is 79,000kg.

Considering that there are 24 ribs per wing, i.e., 48 ribs per aircraft, the lift force per rib can be calculated as:

$$F_{\text{Lift}} = \frac{\text{MTOW} \cdot g}{N_{\text{rib}}}$$

This yields a load on the lower face of 16,130N.

The load on the upper face is determined by the weight of the engine. The LEAP-1A engine has a mass of 3,153kg, corresponding to a distributed force of 30,900N on the upper face. The second engine considered, the CFM-56, has a mass of 2,380kg, corresponding to an upper-face force of 23,324N.

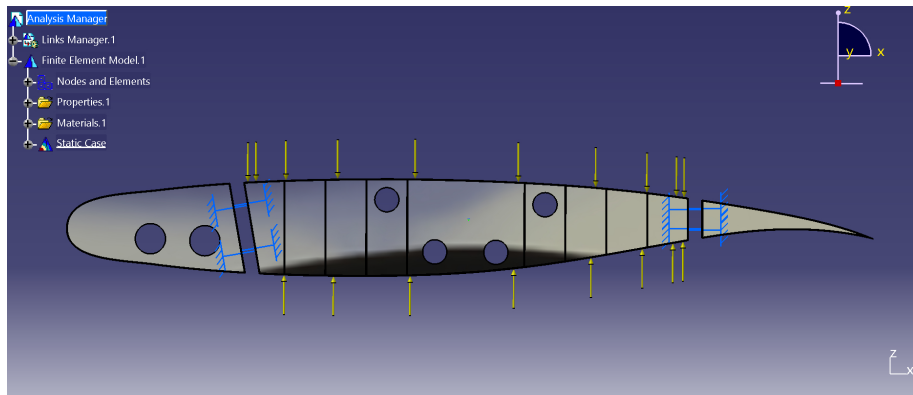


Figure 4.1: Model prepared for the FEA

4.1.3 Mesh size

For each engine, several simulations are performed using tetrahedral meshes. The initial mesh size is set to 50mm, and subsequent simulations are conducted with decreasing mesh sizes in steps of 10mm down to 10mm.

4.2 Simulation and Optimization Results

4.2.1 Results and Optimization for the CFM-56 Engine

Several simulations were conducted for ribs with top/bottom plate and stiffener plate thicknesses ranging from 5mm to 3mm.

The optimization using the Product Engineering Optimizer was performed on the rib with the following characteristics:

Rib thickness	200 mm
Top/bottom thickness	3 mm
Stiffener thickness	3 mm
Stiffener length	60 mm
Stiffener gap	200 mm
Central plate thickness	20 mm
Hole diameter	120 mm
Mass	83 kg

Table 4.2: Rib characteristics used for optimization

During this optimization, the parameters rib thickness, stiffener length, and central plate thickness were left free, with mass as the parameter to minimize. The maximum von Mises stress criterion was set to 220MPa, corresponding to 1.5 times below the 330MPa material limit.

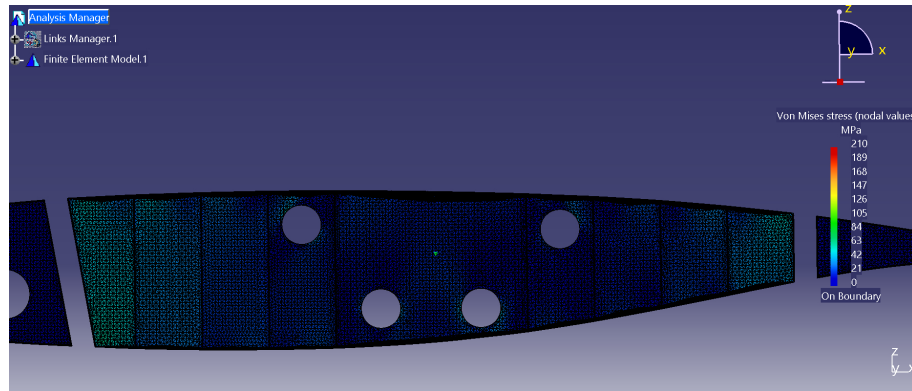


Figure 4.2: Von Mises criterion for CFM-56 engine rib

The characteristics of this rib are presented below 4.3. The mass shown in the table corresponds to the sum of the masses of the three components:

Rib thickness	193.004 mm
Top/bottom thickness	3 mm
Stiffener thickness	3 mm
Stiffener length	48.363 mm
Stiffener gap	200 mm
Central plate thickness	0.468 mm
Hole diameter	120 mm
Mass	20.896 kg

Table 4.3: Optimized rib characteristics for the CFM-56 engine

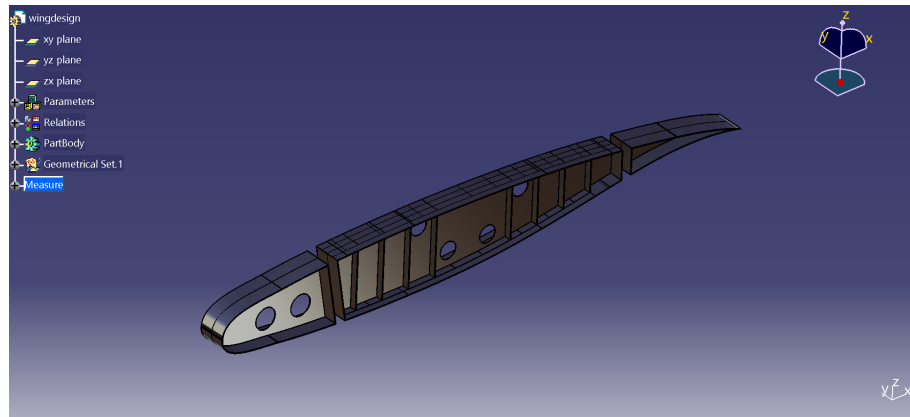


Figure 4.3: Rib design after optimization for the CFM-56

4.2.2 Results and Optimization for the LEAP-1A Engine

Similarly, the rib with the following characteristics was selected as the starting point for the design optimization:

Rib thickness	200 mm
Top/bottom thickness	4 mm
Stiffener thickness	4 mm
Stiffener length	60 mm
Stiffener gap	200 mm
Central plate thickness	20 mm
Hole diameter	120 mm
Mass	88.5 kg

Table 4.4: Initial rib characteristics for optimization of the LEAP-1A engine

Following the same objectives as the previous optimization, the optimized rib design was obtained.

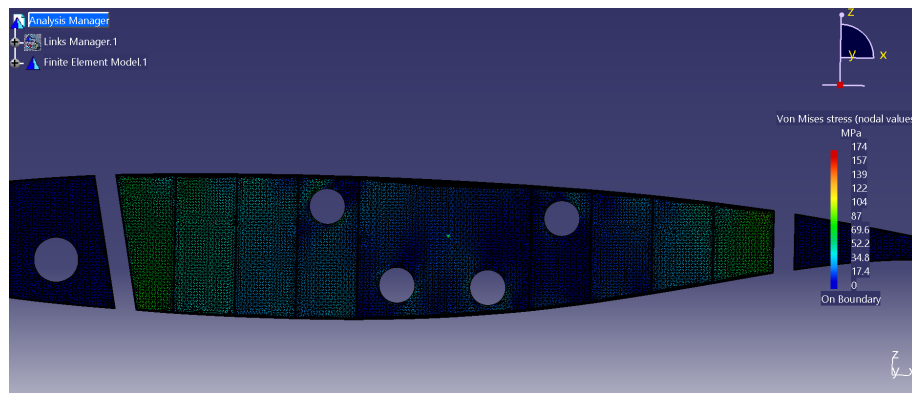


Figure 4.4: Von mises criterion for a Leap-1A engine rib

The optimized rib characteristics for the LEAP-1A engine are presented in Table 4.5:

Rib thickness	191.592 mm
Top/bottom thickness	4 mm
Stiffener thickness	4 mm
Stiffener length	47.596 mm
Stiffener gap	200 mm
Central plate thickness	0.568 mm
Hole diameter	120 mm
Mass	25.708 kg

Table 4.5: Optimized rib characteristics for the LEAP-1A engine

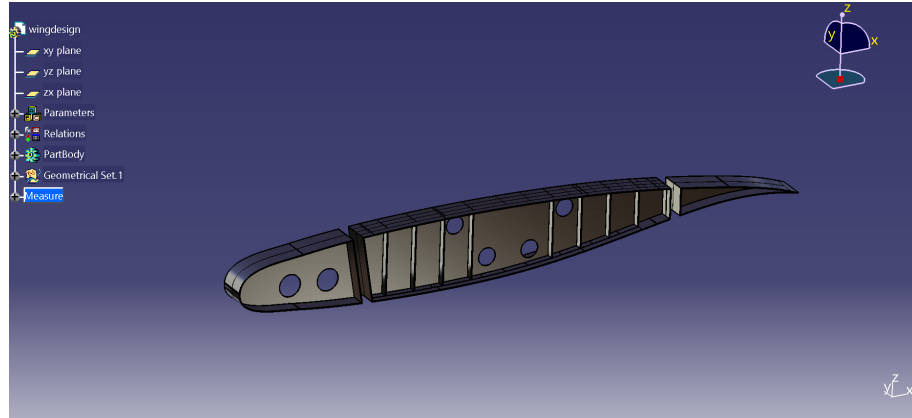


Figure 4.5: Rib design after optimization for the LEAP-1A

4.3 Dimension Standardization for Manufacturing

The two designs obtained using the Product Engineering Optimizer correspond to limit values with a precision that is not realistic for actual manufacturing.

4.3.1 Rib Supporting the LEAP-1A Engine

For the rib simulated with the LEAP-1A engine, new standardized dimensions are proposed:

Rib thickness	192 mm
Top/bottom thickness	4 mm
Stiffener thickness	4 mm
Stiffener length	46 mm
Stiffener gap	200 mm
Central plate thickness	4 mm
Hole diameter	120 mm
Mass	35.5 kg

Table 4.6: Standardized rib dimensions for the LEAP-1A engine

This modification increases the weight slightly but makes the manufacturing of the components more practical. Uniform plate thicknesses reduce the number of operations required and shorten production time.

A new simulation was carried out to verify these updated values.

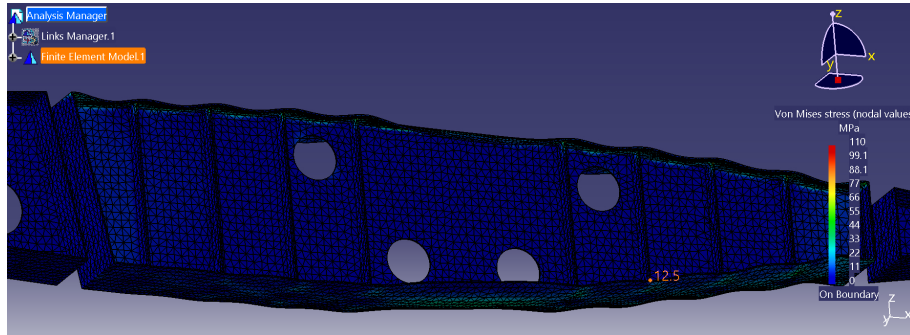


Figure 4.6: Von mises criterion after standardization for Leap-1A engine rib

The final proposed design for modeling and manufacturing the rib supporting the LEAP-1A engine therefore has a mass of 35.5kg.

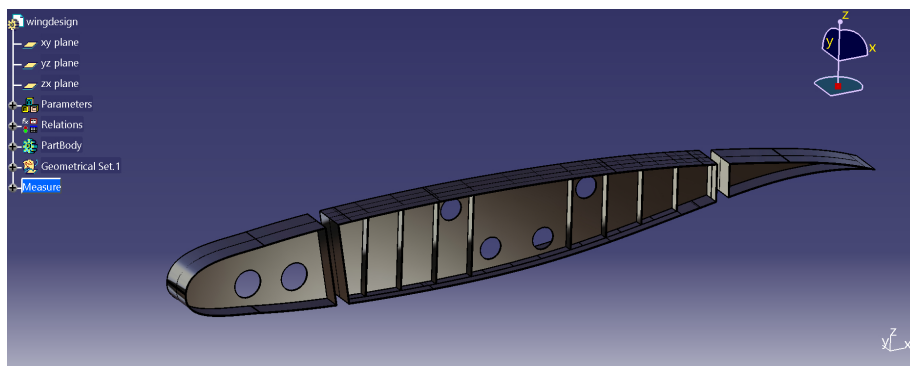


Figure 4.7: Rib design after standardization for the Leap-1A

4.3.2 Rib Supporting the CFM-56 Engine

Similarly, new dimensions are proposed for the rib supporting the CFM-56 engine to make the design more realistic and simplify potential manufacturing.

Rib thickness	193 mm
Top/bottom thickness	3 mm
Stiffener thickness	3 mm
Stiffener length	47 mm
Stiffener gap	200 mm
Central plate thickness	3 mm
Hole diameter	120 mm
Mass	27.1 kg

Table 4.7: Standardized rib dimensions for the CFM-56 engine

A new simulation was performed to verify these updated dimensions.

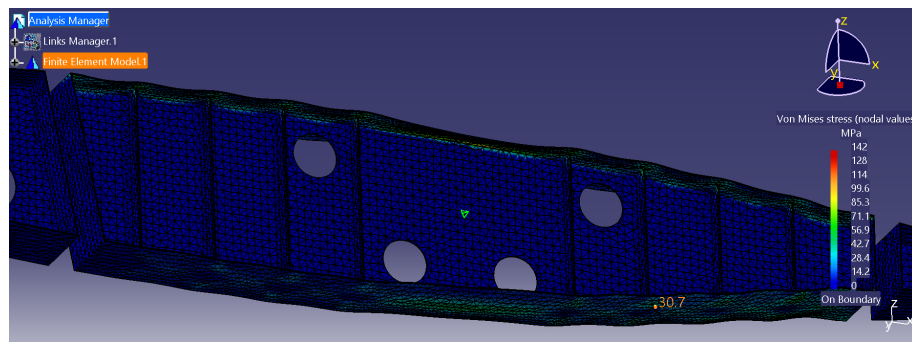


Figure 4.8: Von mises criterion after standardization of the CFM-56 engine rib

The final proposed design for the rib supporting the CFM-56 engine therefore has a mass of 27.1kg.

Chapter 5

Conclusion

5.1 Conclusion

This study focused on modeling and simulating the ribs of the A320 to evaluate the structural impact of increased engine weight. The analysis demonstrated that the mass of the load-bearing rib increased by approximately 7kg, corresponding to a 25% rise, while maintaining structural integrity under operational loads. The final optimized rib designs weigh 27.1kg for the CFM-56 and 35.5kg for the LEAP-1A.

Although this weight increase is notable, it is compensated by a significant improvement in aircraft efficiency, with the A320neo emitting roughly 20% less CO₂ per seat compared to previous-generation models.

Future improvements could involve using more lightweight or open-structure rib designs, as proposed by Krog, Tucker, and Rollema[7]. Applying advanced optimization techniques could also further reduce the wing's mass while still supporting larger engines. These approaches would help achieve a lighter, more efficient wing structure for next-generation commercial aircraft.

References

- [1] Ratnam Steels. Aluminium 2024 T4 / 2024 T351;. Accessed: 2025-11-24. <https://www.ratnamsteels.com/aluminum/aluminium-2024-t4-2024-t351/>.
- [2] Bragado-Aldana E, Riaz A. Assessment of Structurally-Constrained Spanloads for Span-Extended Wing Design. In: AIAA SciTech Forum. Cranfield University, Cranfield, MK43 0AL, United Kingdom: American Institute of Aeronautics and Astronautics; 2024. .
- [3] Magrini A, Benini E, Yao HD, Postma J, Sheaf C. A review of installation effects of ultra-high bypass ratio engines. Progress in Aerospace Sciences. 2020 November;119:100680.
- [4] Teschner, Tom-Robin. CAD & Airframe Design Assignment A25; 2025. Accessed on 24 November 2025. PDF document. Available from: <https://cranfield.instructure.com/courses/37968/modules>.
- [5] Zakuan MAMBM, Aabid A, Khan SA. Modelling and Structural Analysis of Three-Dimensional Wing. International Journal of Engineering and Advanced Technology. 2019 October;9(1):6820-8. Retrieval Number: A2983109119/2019.
- [6] Airbus. A320neo; 2024. Accessed: 2025-11-15. <https://aircraft.airbus.com/en/aircraft/a320-family/a320neo>.
- [7] Krog L, Tucker A, Rollema G. Application of Topology, Sizing and Shape Optimization Methods to Optimal Design of Aircraft Components. Bristol, BS99 7AR: Airbus UK Ltd, Advanced Numerical Simulations Department; 2011. Copyright Altair Engineering, Inc.